Molecular Crystals and Liquid Crystals Science and Technology. Section A. Molecular Crystals and Liquid Crystals

Publication details, including instructions for authors and subscription information:
http://www.tandfonline.com/loi/gmcl19

Synthesis of Antiferromagnetic Macromolecular Particles

Everett E. Carpenter [a], Claudio Sangregorio [a] & Charles J. O'connor [a]

[a] Advanced Materials Research Institute, University of New Orleans, New Orleans, LA, 70148

Version of record first published: 24 Sep 2006

To cite this article: Everett E. Carpenter, Claudio Sangregorio & Charles J. O'connor (1999): Synthesis of Antiferromagnetic Macromolecular Particles, Molecular Crystals and Liquid Crystals Science and Technology. Section A. Molecular Crystals and Liquid Crystals, 334:1, 641-649

To link to this article: http://dx.doi.org/10.1080/10587259908023358

Mol. Cryst. and Liq. Cryst., 1999, Vol. 334, pp. 641-649
Reprints available directly from the publisher
Photocopying permitted by license only

Synthesis of Antiferromagnetic Macromolecular Particles

EVERETT E. CARPENTER, CLAUDIO SANGREGORIO and CHARLES J. O'CONNOR

Advanced Materials Research Institute, University of New Orleans New Orleans, LA 70148

$KMnF_3$ and $NaMnF_3$ in bulk are antiferromagnets with a T_N of 88.3 K and 66 K respectively. Each are easily precipitated by mixing excess NaF or KF and $MnCl_2$. This same reaction can be carried out in the water pools of reverse micelles. By using dioctyl sulfosuccinate (AOT) and isooctane, reverse micelles can be made with a water pool of a specific size controlled by the water/surfactant ratio. This combination of oil phase, surfactant, and aqueous solutions allows a unique opportunity for the fabrication for macromolecular sized materials with narrow size distributions. Using the reverse micelle technique, we synthesized 30 nm particles of $NaMnF_3$ and $KMnF_3$. The particles have a narrow size distribution of <10% verified by TEM. Temperature and field dependent magnetic properties will be discussed.

Keywords: antiferromagnet; reverse micelle; nanoparticles

INTRODUCTION

In the last few decades there has been a growing interest in the synthesis and characterization of particles in the nanometer size region. In fact these materials exhibit in many cases novel and spectacular properties which are intermediate between the molecular ones and those of the correspondent bulk materials. Nanosized magnetic materials have been extensively investigated, since their properties can be employed in a wide range of technological applications[1]. However, despite the large amount of work carried out on ferro-

and ferrimagnetic nanosized materials, only a few works have been published concerning the magnetic properties of antiferromagnetic nanoparticles.

The magnetic behavior of small size grains of antiferromagnetic materials was first proposed by Néel in the early 1960's[2]. He suggested that small particles, due to their high surface/volume ratio, should have a net magnetization below the ordering temperature resulting from uncompensated surface spins. This magnetic moment should give rise to a weak ferromagnetism and a superparamagnetic behavior. In following years the superparamagnetic behavior was experimentally observed in different metal oxide small particles, such as α-Fe_2O_3, Cr_2O_3 and NiO[3]. More recently, the interest in antiferromagnetic materials has grown as a result of interest in quantum tunneling of the magnetization effect[4].

In this paper, we report on the synthesis and magnetic properties of nanosized magnetic particles of alkaline (K or Na) fluoromanganate nanoparticles. Alkaline fluoromanganate materials in bulk exhibit antiferromagnetic behavior with T_N of 65-90K. The nanoparticles were synthesized by using the aqueous core of reverse micelles as a constrained microreactors for the precipitation of the particles[5,6]. Reverse micelles are surfactant aggregates formed by dissolving amphiphilic molecules in organic solvents. Water can be easily solubilized in the polar core of these aggregates, thus forming water droplets dispersed in the organic solvent. Inorganic salt can be dissolved inside the aqueous core of reverse micelles and then can be precipitated, after chemical reaction, as insoluble inorganic nanoparticles. This technique has been proven effective for the synthesis of highly homogeneous nanosized particles of different materials, including metal oxides and superconducting materials[7]. Furthermore, this method has the advantage of providing control over the average size of the particles in a

relatively wide range (3-30 nm) by simply adjusting the water to surfactant molar ratio.

EXPERIMENTAL SECTION

All chemicals were purchased and used without further purification. Bis(2-ethylhexyl) sodium sulfosuccinate (AOT), Potassium Fluoride, Sodium Fluoride, Manganese (II) Chloride, and 2,2,4-trimethylpentane were purchased from Aldrich Chemical (Milwaukee, WI). Distilled and deionized water was used throughout.

Stock solution of 0.65M AOT in isooctane was used in the preparation of the reverse micellar solutions containing the reactants $MnCl_2$ and either KF or NaF. In the preparation of $KMnF_3$, 10 ml of 0.06M $MnCl_2$(aq) were added to 40 ml of AOT in isooctane to form one micellar solution, and 10 ml of 0.18M KF(aq) were added to 40ml of AOT in isooctane to form a second micellar solution. These reactant/AOT solutions were allowed to stir for 5 minutes then were centrifuged for 20 minutes to remove suspended impurities and insolubles. $NaMnF_3$ was synthesized in a similar fashion using NaF instead of KF.

The two reactant/AOT solutions were mixed together while stirring at low speed on a magnetic stir plate. For complete precipitation to $KMnF_3$, the reaction mixture was continuously stirred for about 2 hours. The micelle solution was disrupted with the addition of a large excess of acetone, resulting in a cloudy mixture. The particles were collected by centrifuge. The particles were washed in acetone to ensure the complete removal of the surfactant. The dryed $KMnF_3$ and $NaMnF_3$ powders were pinkish in color.

A Quantum Design MPMS SQUID magnetometer was used for the magnetization measurements. A discussion of general magnetic susceptibility measurements and the calibration techniques are reported elsewhere[8]. TEM images were obtained with a Zeiss 100 microscope. A Phillips-Norelco X-Ray diffractometer with a graphite monochromator and PMT detector was used to obtain XRD plots.

RESULTS AND DISCUSSION

A typical TEM image of the $NaMnF_3$ particles is shown in figure 1. The micrograph clearly shows the occurrence of highly uniform, spherical-shaped

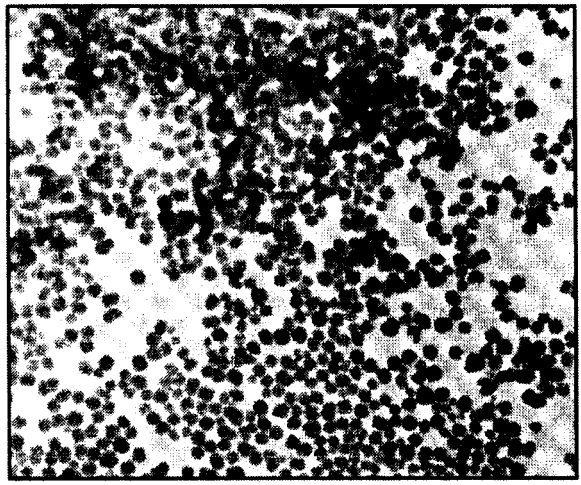

FIGURE 1 Transmission Electron Microscopy micrograph of $NaMnF_3$ particles taken at 37,500x magnification. The bar equals 100 nm.

nanosized particles. The particles are well separated one from each other and their average size is *ca.* 35 nm, with a size variation of less than 10%. TEM images obtained for the $KMnF_3$ sample are very close to those of the sodium compound, showing the occurrence of spherical particles with similar average size.

The X-Ray Diffraction patterns for both $KMnF_3$ (left) and $NaMnF_3$ (right) particles of the prepared samples are shown in figure 2. The left pattern clearly shows all the peaks of a cubic perovskite structure, corresponding to $KMnF_3$, while the right one corresponds to the orthorhombic structure of $NaMnF_3$. In both cases the experimental patterns closely resemble the reference patterns in intensity and position. DCP and EDS elemental analysis experiments confirm the formula given. The evaluation of the particle size

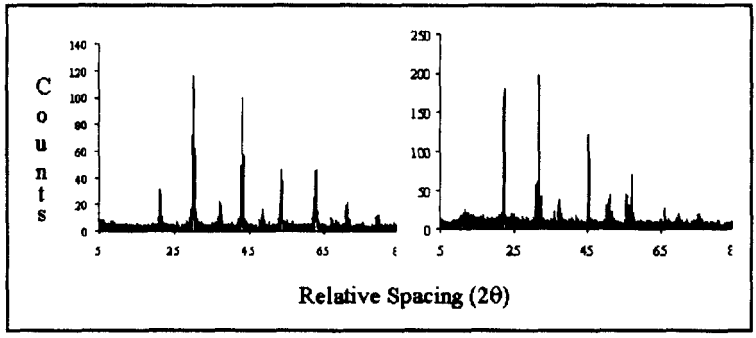

FIGURE 2 X-ray powder diffraction patterns for $KMnF_3$ (left) and $NaMnF_3$ (right) closely resemble their published reference patterns, in intensity and position. The patterns have not been smoothed, only K_α stripped.

from the broadening of the most intense peaks, gives average size of 32 and 37 nm for the K and Na salt, respectively. These values are in good agreement with those obtained by TEM.

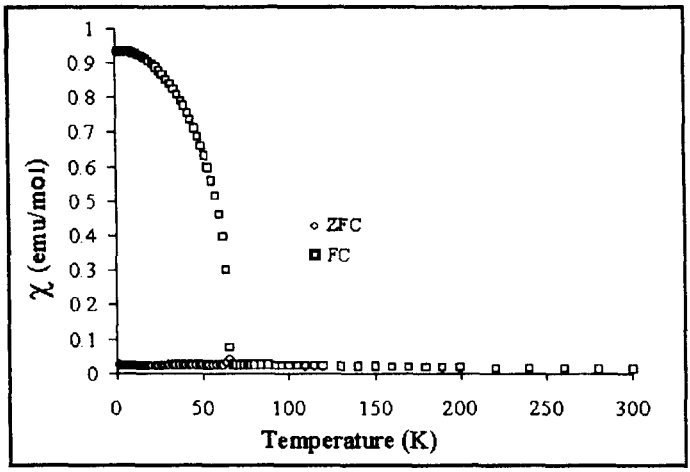

FIGURE 3 Magnetic susceptibility measurements of $NaMnF_3$ samples. The squares indicate field cooled experiment where the sample was cooled to 2K in an applied field of 50 Oe. The circles indicate a zero-field cooled experiment. In both cases the measuring field was 50 Oe.

The temperature dependence of the zero field cooled (ZFC) and field cooled (FC) magnetic susceptibilities of the 35 nm $NaMnF_3$ sample is presented in Figure 3. Above $T=T_N$ the two curves coincide and the magnetic susceptibilities follows a Curie-Weiss law with θ=-157 K, while the magnetic moment of Mn^{2+} ion is 5.51 μ_B. On decreasing temperature the χ *vs.* T curves display some anomalies. At T = 66 K the ZFC curve display a sharp peak but further decreasing temperature the magnetic susceptibility smoothly decreases. This kind of behavior suggests that at T=66 K a transition to a

short-ordered state takes place. An abrupt increase in $\chi(T)$ at or near T_N has been reported for both NH_4MnF_3 and $KMnF_3$ [9,10]. In that case, the authors interpreted this behavior as the presence of spin canting causing weak ferromagnetic behavior. More spectacular is the behavior of the FC curves, which at T=66 K separates from the ZFC curve and strongly increases until, at low temperature, it almost saturates to a value of 0.93 emu/mol. The observed temperature dependence can be explained if we assume that our particles behave like single domain ferromagnetic particles. In other words, we can describe our particles as constituted by an ordered antiferromagnetic (or weak ferromagnetic) core and a surface layer which, due to an incomplete compensation of the surface spins, has a net magnetization. As soon as the sample is cooled through T_N, the particles will be blocked with their magnetic moment frozen along the applied field direction, thus giving rise to a strong increase of the FC susceptibility. However, since good data on the magnetic properties of the bulk compound are not available at the moment, it is not easy to separate the intrinsic weak ferromagnetism of the material from the small size effect on the magnetic properties.

Magnetic hysteresis loops were measured between ±50 kOe for the 35 nm $NaMnF_3$ sample at T=4.5 K, after cooling the sample through the Néel temperature with and without an applied field of 10 kOe. The ZFC hysteresis loop displays a large coercivity of 1700 Oe. The FC hysteresis loop is shown in figure 4. The coercivity is even larger than that observed in the ZFC measurements, being 2350 Oe, while the entire loop is shifted along the applied field direction of 260 Oe. Displacement of FC hysteresis loop is a typical feature of exchange anisotropy in systems where a ferromagnetic spin system is coupled to an antiferromagnetic one[11].

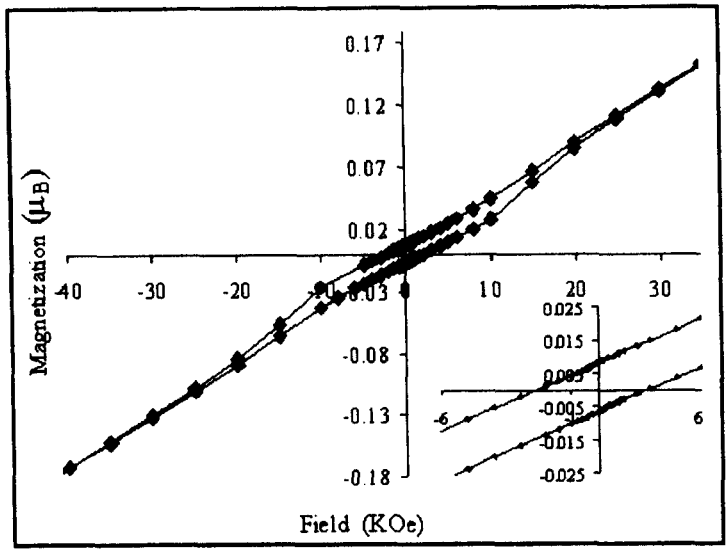

FIGURE 4 Magnetization versus Field measurements were carried out between –50kOe and 50kOe. The inset is enlarged to see the 260 Oe negative bias.

Thus, in our case, the observed shift can be ascribed to the exchange coupling between the ordered antiferromagnetic core and the uncompensated spin shell surrounding the small particles. We point out, to support this interpretation, that a shifted field cooled hysteresis loop has been recently reported for NiO antiferromagnetic particles [12]. A similar shift was observed also in the FC hysteresis curves of $KMnF_3$ nanoparticles, although, both the coercive field and the shift are much lower.

CONCLUSION

Our results show that the microemulsion technique is an effective route for the synthesis of new nanosized antiferromagnetic materials. Although the magnetic properties of these nanosized assemblies have yet to be fully understood, we believe that the obtained results are extremely promising. The study of nanosized antiferromagnetic materials offers a better insight into the fundamental magnetic properties of nanophase materials, which can lead to possible implementation of these materials in devices that currently employ magnetic nanoparticles based on ferromagnetic materials. Work is in progress to synthesis nanoscale particles of various sizes in the range 5-30 nm to investigate the size dependence of the observed properties.

Acknowledgements

This work was supported by the Advanced Materials Research Institute through DARPA grant no. MDA972-97-1-0003. We thank Ms. Joan Wiemann, Dr. Thomas. Kodenkandath, Dr. John Wiley, and Dr. Jinke Tang for powder X-ray diffraction measurements and Mr Al Falster for DCP and EDS elemental analysis.

References

[1] J. Weissmuller, *Nanomaterials: Synthesis, Properties and Applications*(Institute of Physics Publishing, Philadelphia, 1996).

[2] L. Néel, Compt. Rend. **252,** 4075 (1961).

[3] J. Cohen, K. M. Creer, R. Pauthenet, and K. Srivastara, J. Phys. Soc. Japan **17,** 685 (1962).

[4] J. Tejada, R. F. Ziolo, and X. X. Zhang, Chem. Mater. **8,** 1784 (1996).

[5] M.P. Pileni, Journal of Physical Chemistry **97,** 6961–6973 (1993).

[6] H. Wennerstrom, O. Soderman, U. Olsson, and B. Lindman, Colloids and surfaces A. **123–124,** 13–26 (1997).

[7] V. Pillai, P. Kumar, M.J. Hou, P. Ayyub, and D.O. Shah, Adv. Colloid Interface Sci. **55,** 241 (1995).

[8] C.J. O'Connor, Prog. Inorg. Chem. **29,** 202 (1982).

[9] I. Maartense, Solid State Comm **12,** 1133–1136 (1973).

[10] J. Bartolome, R. Burriel, F. Palacio, and D. Gonzalez, Physica **115B,**190–204 (1983).

[11] W.H. Meiklejohn, J. Appl. Phys. **33,** 1328 (1962).

[12] S.A. Makhlouf, F.T. Parker, F.E. Spada, and A.E. Berkowitz, J. Appl. Phys. **81,** 5561 (1997).